ROBUST NEAR-FIELD BEAMFORMING FOR MILLIMETER WAVE COMMUNICATION SYSTEM WITH APERTURE PERTURBATIONS

Gerald C. Nwalozie, Damir Rakhimov, and Martin Haardt

Communications Research Laboratory, Ilmenau University of Technology,
P. O. Box 100565, D-98684 Ilmenau, Germany
Email: {gerald-chetachi.nwalozie, damir.rakhimov, martin.haardt}@tu-ilmenau.de

ABSTRACT

In this paper, we develop a near-field beamforming algorithm that is robust against aperture deformations. We derive analytical expressions on the bounds of the elements of the steering vector as a function of the known bounds of the coordinate displacement. We apply these bounds during the optimization procedure to design beamformers that are robust to aperture perturbations. Simulation results show that the proposed robust near-field beamforming algorithm outperforms the available benchmark in the literature.

***Index Terms*—** robust beamforming, aperture perturbation, near-field beamforming, millimeter frequency range

1. INTRODUCTION

To meet the demands for higher spectral efficiency, employing a large number of antennas in conjunction with the exploitation of higher frequencies has been recognized as a promising solution for future wireless systems [1, 2]. Base stations (BSs) that operate in mmWave frequencies will employ large antenna arrays, as a result of the propagation conditions at these high frequencies [3]. Therefore, this will cause the communicating devices to operate within the BS antenna's near-field or so-called Fresnel region [4]. As a result, the far-field assumption used regularly in conventional wireless systems does not hold. This fact underlies the motivation for the research on near-field beamforming that has recently attracted a lot of attention from the research community. Radiative near-field propagation takes place between the Fraunhofer distance and the Fresnel distance of large-scale antenna arrays operating at mmWave frequencies [5, 6]. The near-field distance can be several dozens of meters for relatively small antennas operating at mmWave and terahertz (THz) frequencies [3, 7].

At the same time, due to the potentially large size of antenna arrays operating at mmWave frequencies, there might be different reasons for the emergence of perturbations in the aperture geometry. For example, these errors might occur during the installation of the antenna array. Because of the size of the antenna array, it is difficult to ensure a perfect aperture geometry during the installation of the antenna, which might consist of multiple panels being stacked together. This leads to inevitable aperture deformations that degrade the overall performance of the communication system. For instance, the change of curvature influences the antenna directivity and the level of the sidelobes [8, 9].

Most of the conventional methods for robust beamforming are designed for far-field scenarios. Moreover, most of them are focused on the robustness against the steering vector mismatch, which is caused by the estimation error of the angle of arrival (AoA) or angle of departure (AoD) [10, 11, 12]. For example, the authors in [10] proposed a robust algorithm based on the prior information about the bound on the steering vector mismatch to avoid self-nulling of the desired signal even in the case of worst-case perturbations. On the other hand, the authors in [13] considered the beamforming design robust to aperture deformations caused by thermal distortions. Unfortunately, this work has a limited application for the problem we consider, since the system model is based on the far-field assumption and considers the non-terrestrial networks. There are also few references related to the design of robust beamforming for near-field users. The authors in [14] proposed a near-field beamforming algorithm robust to steering vector mismatches, which is a similar problem to [10]. In [15], the authors proposed a near-field beamforming algorithm with robustness against distance errors. However, even though there are many excellent references on the topic of robust beamforming design, the number of publications for the implementation of robust beamforming methods for near-field users with respect to aperture deformations stays rather limited.

In this paper, we consider robust near-field beamforming for mmWave networks under aperture perturbations of the base station (BS) antenna array. We cast the problem as a worst-case optimization problem that can be solved using available off-the-shelf tools. To this end, for the considered near-field model we derive a closed-form expression for the bounds on the norms of the perturbations of the array steering vector as a function of the bound on the coordinate displacements.

2. SYSTEM MODEL

We consider a downlink multi-user MIMO system where the BS is equipped with a uniform rectangular array (URA) x-y plane consisting of M_x and M_y antennas along the $X-$ and $Y-$ directions such that $M = M_\text{x} \cdot M_\text{y}$ is the total number of BS antennas. We assume that the phase center of the BS antenna array is at the origin of the coordinate system. The inter-element spacing between the elements along the x-axis and the y-axis is denoted as Δ_x and Δ_y, respectively.

The BS serves a single antenna user equipment (UE) in the radiative near-field of the BS. The spherical coordinates of the UE are given as $(\theta_\text{rx}, \phi_\text{rx}, r_\text{rx})$, where θ_rx and ϕ_rx are the azimuth and elevation angles in the direction of the phase center of the transmitter, while r_rx is the distance towards it. The received signal at the UE can be written as

$$y(k) = \boldsymbol{w}^\mathsf{H}\boldsymbol{x}(k), \tag{1}$$

where $\boldsymbol{w} \in \mathbb{C}^{M\times 1}$ is denotes the vector of beamforming weights, $\boldsymbol{x}(k) \in \mathbb{C}^{M\times 1}$ is the input vector, and k denotes the time index. The input vector can be described as

$$\boldsymbol{x}(k) = \boldsymbol{a}s(k) + \boldsymbol{i}(k) + \boldsymbol{n}(k) \tag{2}$$

where $\boldsymbol{a} = \text{vec}\{\boldsymbol{A}\} \in \mathbb{C}^{M\times 1}$ is the vectorization of the near-field steering matrix $\boldsymbol{A} \in \mathbb{C}^{M_\text{x}\times M_\text{y}}$ comprising the response between every element of the BS antenna array and the UE. Furthermore, $s(k)$ is the desired signal, $\boldsymbol{i}(k)$ is the interference, and $\boldsymbol{n}(k) \in \mathbb{C}^{M\times 1}$ is the noise assumed as zero-mean circularly symmetric complex Gaussian.

The (m_x, m_y) element of the near-field steering matrix $\boldsymbol{A}$ where $0 \leq m_\text{x} \leq M_\text{x}-1,\ 0 \leq m_\text{y} \leq M_\text{y}-1$ can be described as

$$\boldsymbol{A}(m_\text{x}, m_\text{y}) = \frac{1}{\delta_{m_\text{x},m_\text{y}}} e^{-j\frac{2\pi}{\lambda}\delta_{m_\text{x},m_\text{y}}} \in \mathbb{C}, \tag{3}$$

where $\delta_{m_\text{x},m_\text{y}}$ is the distance between the (m_x, m_y) element of the BS antenna array and the receive antenna given as

$$\delta_{m_\text{x},m_\text{y}} = \sqrt{(x_\text{rx} - m_\text{x}\Delta_\text{x})^2 + (y_\text{rx} - m_\text{y}\Delta_\text{y})^2 + (z_\text{rx} - 0)^2} \tag{4}$$

where $(x_\text{rx}, y_\text{rx}, z_\text{rx})$ represent the cartesian coordinates of the UE, which are respectively given as $x_\text{rx} = r_\text{rx}\cos\phi_\text{rx}\sin\theta_\text{rx}$, $y_\text{rx} = r_\text{rx}\sin\phi_\text{rx}\sin\theta_\text{rx}$, and $z_\text{rx} = r_\text{rx}\cos\theta_\text{rx}$. Using a first order approximation, (4) can be further simplified as

$$\begin{aligned}\delta_{m_\text{x},m_\text{y}} &= L_\text{rx}\sqrt{1 - \frac{2m_\text{x}\Delta_\text{x}x_\text{rx} + 2m_\text{y}\Delta_\text{y}y_\text{rx} - m_\text{x}^2\Delta_\text{x}^2 - m_\text{y}^2\Delta_\text{y}^2}{L_\text{rx}^2}} \\ &\approx L_\text{rx} - \frac{2m_\text{x}\Delta_\text{x}x_\text{rx} - m_\text{x}^2\Delta_\text{x}^2}{2L_\text{rx}} - \frac{2m_\text{y}\Delta_\text{y}y_\text{rx} - m_\text{y}^2\Delta_\text{y}^2}{2L_\text{rx}},\end{aligned} \tag{5}$$

where $L_\text{rx} = \sqrt{x_\text{rx}^2 + y_\text{rx}^2 + z_\text{rx}^2}$ and we used the approximation $\sqrt{1+x} \approx 1 + \frac{x}{2}$ for small x.

2.1. Aperture Perturbation Model

In this section, we introduce the BS antenna array aperture perturbation model and describe its impact on the components of the received signal given in (1). One of the possible causes of aperture perturbation may be as a result of imperfect installation of the antenna array. We use a deterministic uncertainty region model in which the error is bounded. We assume that the imperfections due to aperture perturbation lead to a displacement in the (x, y, z) coordinates of the elements of the BS antenna array. We assume that different coordinates are uncorrelated, while the perturbation of one coordinate can be defined by the corresponding known bound.

Let us denote $\boldsymbol{\sigma} = [\sigma_\text{x}, \sigma_\text{y}, \sigma_\text{z}]^\mathsf{T} \in \mathbb{R}^3$ as a vector that contains the known bounds of the perturbation for each axis. In this paper, we assume that the displacements for the x and y coordinates are much smaller in comparison to the displacement for the z coordinate, i.e., $\sigma_\text{z} \gg \sigma_\text{x} \approx \sigma_\text{y}$. On the other hand, the uncertainty region can be described as an ellipsoid of known shape [12]. The uncertainty ellipse $\mathcal{E}$ for the vector displacement $\boldsymbol{p} \in \mathbb{R}^3$ is defined as $\mathcal{E}_p = \{\text{diag}(\boldsymbol{\sigma}) \cdot \boldsymbol{u}\ ||\|\boldsymbol{u}\| \leq 1,\ \boldsymbol{u} \in \mathbb{R}^3\}$. We assume that we have information only about the statistics of the perturbation but not the instantaneous realizations of them. The (m_x, m_y) element of the steering matrix of the input signal affected by the perturbations is given by

$$\tilde{\boldsymbol{A}}(m_\text{x}, m_\text{y}) = \frac{1}{\tilde{\delta}_{m_\text{x},m_\text{y}}} e^{-j\frac{2\pi}{\lambda}\tilde{\delta}_{m_\text{x},m_\text{y}}} \in \mathbb{C}, \tag{6}$$

where $\tilde{\delta}_{m_\text{x},m_\text{y}}$ is defined as

$$\tilde{\delta}_{m_\text{x},m_\text{y}} = \sqrt{a^2 + b^2 + c^2}, \tag{7}$$

and $a = (x_\text{rx} - m_\text{x}\Delta_\text{x} + p^{\text{err},x}_{m_\text{x},m_\text{y}})$, $b = (y_\text{rx} - m_\text{y}\Delta_\text{y} + p^{\text{err},y}_{m_\text{x},m_\text{y}})$, and $c = (z_\text{rx} - 0 + p^{\text{err},z}_{m_\text{x},m_\text{y}})$ with $p^{\text{err},i}_{m_\text{x},m_\text{y}}$ being the random displacement along the i axis, $i \in \{\text{x}, \text{y}, \text{z}\}$. Similarly, using a first order approximation we can approximate $\tilde{\delta}_{m_\text{x},m_\text{y}}$ as

$$\begin{aligned}\tilde{\delta}_{m_\text{x},m_\text{y}} &= L_\text{rx}\sqrt{1 - \frac{2m_\text{x}\Delta_\text{x}x_\text{rx} + 2m_\text{y}\Delta_\text{y}y_\text{rx} - m_\text{x}^2\Delta_\text{x}^2 - m_\text{y}^2\Delta_\text{y}^2 + \xi^\text{err}_{m_\text{x},m_\text{y}}}{L_\text{rx}^2}} \\ &\approx L_\text{rx} - \frac{2m_\text{x}\Delta_\text{x}x_\text{rx} - m_\text{x}^2\Delta_\text{x}^2}{2L_\text{rx}} - \frac{2m_\text{y}\Delta_\text{y}y_\text{rx} - m_\text{y}^2\Delta_\text{y}^2}{2L_\text{rx}} - \frac{\xi^\text{err}_{m_\text{x},m_\text{y}}}{2L_\text{rx}} \\ &\approx \delta_{m_\text{x},m_\text{y}} + \Delta\delta_{m_\text{x},m_\text{y}}\end{aligned} \tag{8}$$

where $\Delta\delta_{m_\text{x},m_\text{y}} = -\frac{\xi^\text{err}_{m_\text{x},m_\text{y}}}{2L_\text{rx}}$ and
$\xi^\text{err}_{m_\text{x},m_\text{y}} = 2(x_\text{rx} - m_\text{x}\Delta_\text{x})p^{\text{err,x}}_{m_\text{x},m_\text{y}} + 2(y_\text{rx} - m_\text{y}\Delta_\text{y})p^{\text{err,y}}_{m_\text{x},m_\text{y}} + 2(z_\text{rx} - 0)p^{\text{err,z}}_{m_\text{x},m_\text{y}}$.
Next, we compute the first-order Taylor expansion for small perturbations given as

$$e^{j(\alpha+\Delta\alpha)} = e^{j\alpha} + j\Delta\alpha e^{j\alpha} + \mathcal{O}(\Delta^2) \approx e^{j\alpha} + \Delta_\alpha, \tag{9}$$

where $\Delta_\alpha = j\Delta\alpha e^{j\alpha}$. Then by applying (9) to (6), we can find the first-order Taylor approximation for the expression of the perturbed matrix $\tilde{\boldsymbol{A}}$ as given in (10) on top of the next page, where $\Delta\boldsymbol{A}(m_\text{x}, m_\text{y}) = -j\frac{2\pi}{\lambda}\Delta\delta_{m_\text{x},m_\text{y}}\boldsymbol{A}(m_\text{x}, m_\text{y})$. We assume that the effect of aperture perturbations on the amplitude is much smaller than on the phase.

Additionally, we represent the expression in vector format after back substitution as given in (11) on top of the next page,

$$\tilde{\boldsymbol{A}}(m_{\mathrm{x}},m_{\mathrm{y}}) \approx \frac{1}{\delta_{m_{\mathrm{x}},m_{\mathrm{y}}}} e^{j\frac{2\pi}{\lambda}(\delta_{m_{\mathrm{x}},m_{\mathrm{y}}}+\Delta\delta_{m_{\mathrm{x}},m_{\mathrm{y}}})} \approx \frac{1}{\delta_{m_{\mathrm{x}},m_{\mathrm{y}}}} e^{-j\frac{2\pi}{\lambda}\delta_{m_{\mathrm{x}},m_{\mathrm{y}}}} - j\frac{2\pi}{\lambda}\frac{\Delta\delta_{m_{\mathrm{x}},m_{\mathrm{y}}}}{\delta_{m_{\mathrm{x}},m_{\mathrm{y}}}} e^{-j\frac{2\pi}{\lambda}\delta_{m_{\mathrm{x}},m_{\mathrm{y}}}} = \boldsymbol{A}(m_{\mathrm{x}},m_{\mathrm{y}}) + \Delta\boldsymbol{A}(m_{\mathrm{x}},m_{\mathrm{y}}), \quad (10)$$

$$\Delta\boldsymbol{A}(m_{\mathrm{x}},m_{\mathrm{y}}) = j\frac{2\pi}{\lambda}\left[\frac{(x_{\mathrm{rx}}-m_{\mathrm{x}}\Delta_{\mathrm{x}})}{L_{\mathrm{rx}}},\ \frac{(y_{\mathrm{rx}}-m_{\mathrm{y}}\Delta_{\mathrm{y}})}{L_{\mathrm{rx}}},\ \frac{z_{\mathrm{rx}}}{L_{\mathrm{rx}}}\right]\cdot\left[p^{\mathrm{err},x}_{m_{\mathrm{x}},m_{\mathrm{y}}},\ p^{\mathrm{err},y}_{m_{\mathrm{x}},m_{\mathrm{y}}},\ p^{\mathrm{err},z}_{m_{\mathrm{x}},m_{\mathrm{y}}}\right]^{\mathsf{T}}\cdot\boldsymbol{A}(m_{\mathrm{x}},m_{\mathrm{y}}) = \boldsymbol{q}^{\mathsf{T}}_{m_{\mathrm{x}},m_{\mathrm{y}}}\boldsymbol{p}_{m_{\mathrm{x}},m_{\mathrm{y}}}\boldsymbol{A}(m_{\mathrm{x}},m_{\mathrm{y}}) \quad (11)$$

---

where $\boldsymbol{q}_{m_{\mathrm{x}},m_{\mathrm{y}}}$ and $\boldsymbol{p}_{m_{\mathrm{x}},m_{\mathrm{y}}}$, are respectively define as

$$\boldsymbol{q}_{m_{\mathrm{x}},m_{\mathrm{y}}} = j\frac{2\pi}{\lambda}\left[\frac{(x_{\mathrm{rx}}-m_{\mathrm{x}}\Delta_{\mathrm{x}})}{L_{\mathrm{rx}}},\ \frac{(y_{\mathrm{rx}}-m_{\mathrm{y}}\Delta_{\mathrm{y}})}{L_{\mathrm{rx}}},\ \frac{z_{\mathrm{rx}}}{L_{\mathrm{rx}}}\right]^{\mathsf{T}},$$
$$\boldsymbol{p}_{m_{\mathrm{x}},m_{\mathrm{y}}} = \left[p^{\mathrm{err},x}_{m_{\mathrm{x}},m_{\mathrm{y}}},\ p^{\mathrm{err},y}_{m_{\mathrm{x}},m_{\mathrm{y}}},\ p^{\mathrm{err},z}_{m_{\mathrm{x}},m_{\mathrm{y}}}\right]^{\mathsf{T}}.$$

After that, we find the bound on the norm of the mismatch of each element of the near-field steering matrix $\boldsymbol{A}$ caused by aperture perturbation with a known norm of the bound of error $\|\boldsymbol{p}_{m_{\mathrm{x}},m_{\mathrm{y}}}\|_2 \in \mathcal{E}_p$. The bound on the norm of the mismatch is given as

$$\begin{aligned}\|\Delta\boldsymbol{A}(m_{\mathrm{x}},m_{\mathrm{y}})\|_2 &= \sqrt{\Delta\boldsymbol{A}^*(m_{\mathrm{x}},m_{\mathrm{y}})\Delta\boldsymbol{A}(m_{\mathrm{x}},m_{\mathrm{y}})}\\ &= \sqrt{\boldsymbol{A}^*(m_{\mathrm{x}},m_{\mathrm{y}})\boldsymbol{q}^{\mathsf{H}}_{m_{\mathrm{x}},m_{\mathrm{y}}}\boldsymbol{p}^*_{m_{\mathrm{x}},m_{\mathrm{y}}}\boldsymbol{p}^{\mathsf{T}}_{m_{\mathrm{x}},m_{\mathrm{y}}}\boldsymbol{q}_{m_{\mathrm{x}},m_{\mathrm{y}}}\boldsymbol{A}(m_{\mathrm{x}},m_{\mathrm{y}})}\\ &\le \frac{1}{\delta_{m_{\mathrm{x}},m_{\mathrm{y}}}}\|\boldsymbol{\sigma}\|_2\|\boldsymbol{q}_{m_{\mathrm{x}},m_{\mathrm{y}}}\|_2 = \epsilon_{m_{\mathrm{x}},m_{\mathrm{y}}},\end{aligned} \quad (12)$$

where we apply the *Cauchy-Bunyakovsky-Schwarz* inequality for inner products, i.e., $\|\boldsymbol{b}^{\mathsf{H}}\boldsymbol{d}\|_2 \le \|\boldsymbol{b}\|_2\cdot\|\boldsymbol{d}\|_2,\ \forall\boldsymbol{b},\boldsymbol{d}\in\mathbb{C}^m$ and use the substitution $\boldsymbol{p} = \mathrm{diag}(\boldsymbol{\sigma})\cdot\boldsymbol{u},\ \|\boldsymbol{u}\|\le 1$.

3. PROBLEM FORMULATION

The signal-to-interference-plus-noise ratio (SINR) at the receiver is defined as [16]

$$\mathrm{SINR} = \frac{\sigma_{\mathrm{s}}^2|\boldsymbol{w}^{\mathsf{H}}\boldsymbol{a}|^2}{\boldsymbol{w}^{\mathsf{H}}\boldsymbol{R}_{i+n}\boldsymbol{w}}, \quad (13)$$

where $\boldsymbol{R}_{i+n} = \mathbb{E}\{[\boldsymbol{i}(k)+\boldsymbol{n}(k)][\boldsymbol{i}(k)+\boldsymbol{n}(k)]^{\mathsf{H}}\}\in\mathbb{C}^{M\times M}$ is the interference-plus-noise covariance matrix, σ_s^2 is the signal power, and $\mathbb{E}\{\cdot\}$ denotes the statistical expectation. The optimal weight vector can be found via a maximization of the SINR in (13) which is equivalently formulated as follows:

$$\min_{\boldsymbol{w}}\quad \boldsymbol{w}^{\mathsf{H}}\boldsymbol{R}_{i+n}\boldsymbol{w}\quad \text{s. t.}\quad \boldsymbol{w}^{\mathsf{H}}\boldsymbol{a}=1. \quad (14)$$

Due to the unavailability of the true interference-plus-noise covariance matrix in practice, the matrix is commonly replaced by the sample covariance matrix as

$$\hat{\boldsymbol{R}} = \frac{1}{N_{\mathrm{s}}}\sum_{k=1}^{N_{\mathrm{s}}}\boldsymbol{x}(k)\boldsymbol{x}(k)^{\mathsf{H}}. \quad (15)$$

Therefore, it is possible to write problem (14) as

$$\min_{\boldsymbol{w}}\ \boldsymbol{w}^{\mathsf{H}}\hat{\boldsymbol{R}}\boldsymbol{w} \quad (16a)$$
$$\text{s. t. } \boldsymbol{w}^{\mathsf{H}}\boldsymbol{a}=1. \quad (16b)$$

However, the solution to problem (16a) lacks the necessary robustness to handle a mismatch between the presumed and actual steering vectors. In the following, we develop a new robust near-field beamformer that takes into account the prior information about the bound on the perturbation of the $(m_{\mathrm{x}},m_{\mathrm{y}})$ element of the steering matrix $\boldsymbol{A}$. We denote the actual steering vector comprising the effect of the random perturbations of the surface on the BS antenna array as $\tilde{\boldsymbol{a}}$. The relationship between the actual and the presumed steering vector is given as [10]

$$\tilde{\boldsymbol{a}} = \boldsymbol{a} + \boldsymbol{\delta}_{\mathrm{err}}, \quad (17)$$

where $\boldsymbol{a} = \mathrm{vec}(\boldsymbol{A})$ and the vector $\boldsymbol{\delta}_{\mathrm{err}}\in\mathbb{C}^{M\times 1}$ models the effect of the random perturbations on the steering vector due to aperture perturbations. The norm of the error vector is bounded by γ, i.e., $\|\boldsymbol{\delta}_{\mathrm{err}}\|\le\gamma$ where γ is obtained from (12) as $\gamma = \sqrt{M}\max(\epsilon_m), \forall m\in M$ which represents the worst-case bound on the perturbations. Next, we denote $\mathcal{A}$ as the set of all possible realizations of the steering vector impacted by the random perturbations

$$\mathcal{A} = \{\boldsymbol{c}|\boldsymbol{c}=\boldsymbol{a}+\boldsymbol{e},\ \|\boldsymbol{e}\|\le\gamma\}. \quad (18)$$

As in [10], we assume that $\boldsymbol{\delta}_{\mathrm{err}} = \boldsymbol{e}$ and as a result we impose the following constraint $|\boldsymbol{w}^{\mathsf{H}}\boldsymbol{c}|\ge 1,\ \forall\boldsymbol{c}\in\mathcal{A}$, which implies that for all vectors that belong $\mathcal{A}$ that the absolute value of the array response should not be smaller than one. Therefore, the robust near-field beamforming that tries to maximize the SINR for the worst-case perturbation in the case of steering vector mismatch can be written as

$$\min_{\boldsymbol{w}}\quad \boldsymbol{w}^{\mathsf{H}}\hat{\boldsymbol{R}}\boldsymbol{w}, \quad (19a)$$
$$\text{s. t.}\quad |\boldsymbol{w}^{\mathsf{H}}\boldsymbol{c}|\ge 1,\ \forall\boldsymbol{c}\in\mathcal{A}, \quad (19b)$$

where (19) designs the beamforming weight by minimizing the worst-case output power subject to the distortionless response constraint which must be satisfied for the steering vector bounded by the worst-case norm $\boldsymbol{\delta}_{\mathrm{err}}$. The nonlinear constraint in (19b) can be equivalently written as

$$\min_{\boldsymbol{e}\in\mathcal{D}(\gamma)}|\boldsymbol{w}^{\mathsf{H}}(\boldsymbol{a}+\boldsymbol{e})|\ge 1, \quad (20)$$

where the set $\mathcal{D}(\gamma)\triangleq\{\boldsymbol{e}|\,\|\boldsymbol{e}\|\le\gamma\}$. Following [10], we can show that the vector that achieves the minimum can be found by solving the problem

$$|\boldsymbol{w}^{\mathsf{H}}(\boldsymbol{a}+\boldsymbol{e})| = |\boldsymbol{w}^{\mathsf{H}}\boldsymbol{a}| - \gamma\|\boldsymbol{w}\|, \quad (21)$$

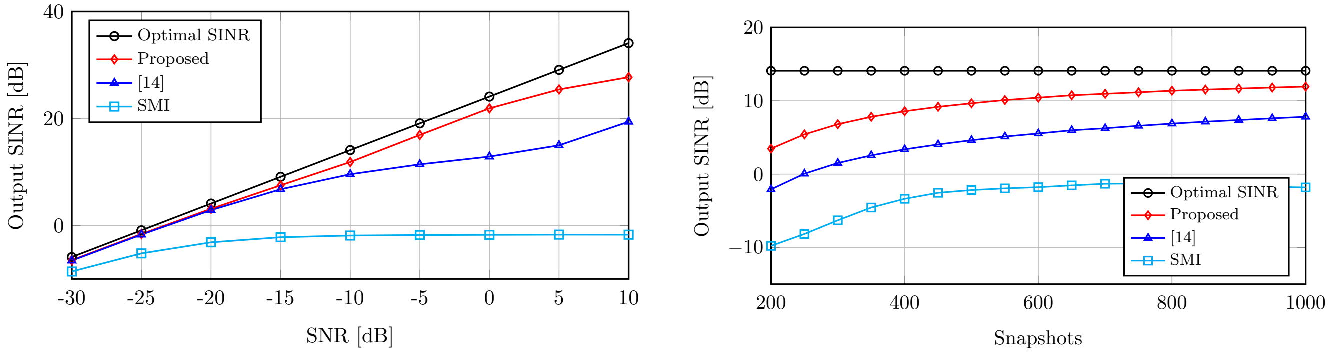

(a) Output SINR versus SNR, $N_s = 1000$.

(b) Output SINR versus N_s, SNR= -10 dB.

Fig. 1: Simulation results for Robust near-field beamforming with Aperture perturbations.

such that the solution with respect to the vector $\boldsymbol{e}$ can be written as $\boldsymbol{e} = -\frac{\boldsymbol{w}}{\|\boldsymbol{w}\|}\gamma e^{j\phi}$, where $\phi = \angle(\boldsymbol{w}^\mathsf{H}\boldsymbol{a})$. From [10], it is required that $|\boldsymbol{w}^\mathsf{H}\boldsymbol{a}| \geq \gamma\|\boldsymbol{w}\|$, otherwise the white noise gain of the robust beamformer may be insufficient, where the white noise gain is the array gain when the noise term $\boldsymbol{z}$ is spatially white. Therefore, the constraint in (19b) can be replaced by

$$|\boldsymbol{w}^\mathsf{H}\boldsymbol{a}| - \gamma\|\boldsymbol{w}\| \geq 1. \tag{22}$$

Then, the worst-case robust near-field beamforming problem can be formulated as the following optimization problem

$$\min_{\boldsymbol{w}} \boldsymbol{w}^\mathsf{H}\hat{\boldsymbol{R}}\boldsymbol{w} \tag{23a}$$

$$\text{s. t. } |\boldsymbol{w}^\mathsf{H}\boldsymbol{a}| - \gamma\|\boldsymbol{w}\| \geq 1. \tag{23b}$$

Since the cost function of (23a) is unchanged when $\boldsymbol{w}$ undergoes an arbitrary phase rotation [10], then the problem can be rewritten as

$$\min_{\boldsymbol{w}} \boldsymbol{w}^\mathsf{H}\hat{\boldsymbol{R}}\boldsymbol{w} \tag{24a}$$

$$\text{s. t. } \boldsymbol{w}^\mathsf{H}\boldsymbol{a} \geq \gamma\|\boldsymbol{w}\| + 1,\ \text{Im}\{\boldsymbol{w}^\mathsf{H}\boldsymbol{a}\} = 0. \tag{24b}$$

Since the optimization problem (24) is convex, it can easily be reformulated as a second-order cone program (SOCP) similar to [10, 14] which can be solved using interior point methods with a complexity of $\mathcal{O}(M^{3.5})$ [17].

4. NUMERICAL RESULTS

In this section, we show simulation results to evaluate the performance of the proposed and existing algorithms. We assume that the BS uses a URA with $M_\text{x} = 64$ and $M_\text{y} = 4$ antennas which are uniformly spaced. For simplicity we assume that $\Delta_\text{x} = \Delta_\text{y} = \Delta = \lambda/2$ at a carrier frequency of 28 GHz. The azimuth and elevation angles of the desired UE are given as $\{90°,\ 45°\}$. We assume that there are two interferers whose azimuth and elevation angles are respectively given as $\{50°,\ 120°\}$ and $\{120°,\ 90°\}$. The interference-to-noise ratio is 30 dB. The UEs are uniformly spaced in the radiative near-field of the BS antenna.

The proposed algorithm is compared with the optimal solution (optimal SINR) given as $\text{SINR}_\text{opt} = \sigma_\text{s}^2\tilde{\boldsymbol{a}}^\mathsf{H}\boldsymbol{R}_{i+n}\tilde{\boldsymbol{a}}$ according to [18], the sample matrix inversion (SMI) beamforming scheme, and the worst-case near-field beamforming design with a mismatch in the steering vector due to AoA errors according to [14]. In our simulations, the known bounds on the norm of the perturbations for each of the axes are given as $(0.01\lambda, 0.01\lambda, 0.05\lambda)$, for the steering vector mismatch algorithm we modified the known bound given in [14], to take into account the number of sensors, $\epsilon = c\sqrt{M}, c = 0.01$.

Fig. 1a shows the SINR performance over the SNR for $N_s = 1000$ samples. The result is averaged over 1000 realizations. From the figure, it is observed that the proposed robust near-field beamforming has a better performance compared to the existing benchmark [14] and the SMI scheme.

In Fig. 1b the output SINR as a function of the number of snapshots are presented. The considered SNR is -10 dB, and the result is averaged over 1000 realizations. Here the comparison of the convergence of the proposed robust near-field beamforming algorithm and the existing schemes is demonstrated. The proposed algorithm outperforms the existing solutions.

5. CONCLUSIONS

In this paper, we have proposed a robust near-field beamforming algorithm. The proposed algorithm demonstrated robustness due to BS antenna array aperture perturbations. We analytically derive the bounds on the perturbations of the steering vector as a function of the known norm of the coordinate displacements. The simulation results confirm that the proposed robust near-field algorithm outperforms the benchmark schemes.

ACKNOWLEDGMENTS

This work was supported by Nnamdi Azikiwe University Nigeria, under NEEDS Assessment Fund and the Communication Research Laboratory, Ilmenau University of Technology, Germany.

6. REFERENCES

[1] E. De Carvalho, A. Ali, A. Amiri, M. Angjelichinoski, and R. W. Heath, “Non-stationarities in extra-large-scale massive MIMO,” *IEEE Wireless Communications*, vol. 27, no. 4, pp. 74–80, 2020.

[2] M. Giordani, M. Polese, M. Mezzavilla, S. Rangan, and M. Zorzi, “Toward 6G networks: Use cases and technologies,” *IEEE Communications Magazine*, vol. 58, no. 3, pp. 55–61, 2020.

[3] J. Zhang, E. Björnson, M. Matthaiou, D. W. K. Ng, H. Yang, and D. J. Love, “Prospective multiple antenna technologies for beyond 5G,” *IEEE Journal on Selected Areas in Communications*, vol. 38, no. 8, pp. 1637–1660, 2020.

[4] M. Cui, Z. Wu, Y. Lu, X. Wei, and L. Dai, “Near-field MIMO communications for 6G: Fundamentals, challenges, potentials, and future directions,” *IEEE Communications Magazine*, vol. 61, no. 1, pp. 40–46, 2022.

[5] K. T. Selvan and R. Janaswamy, “Fraunhofer and fresnel distances : Unified derivation for aperture antennas,” *IEEE Antennas and Propagation Magazine*, vol. 59, no. 4, pp. 12–15, 2017.

[6] H. Zhang, N. Shlezinger, F. Guidi, D. Dardari, M. F. Imani, and Y. C. Eldar, “Beam focusing for near-field multiuser MIMO communications,” *IEEE Transactions on Wireless Communications*, vol. 21, no. 9, pp. 7476–7490, 2022.

[7] G. C. Nwalozie, D. Rakhimov, and M. Haardt, “Near-field beamforming for MU-MIMO millimeter wave communication system,” in *Proc. of 31st European Signal Processing Conference (EUSIPCO 2023), Helsinki, Finland*, September 2023.

[8] Y. Rahmat-Samii, “Effects of deterministic surface distortions on reflector antenna performance,” *Annales des télécommunications*, vol. 40, pp. 350–360, 1985.

[9] R. Sharp, M. Liao, J. Giriunas, J. Heighway, A. Lagin, and R. Steinbach, “Reflector surface distortion analysis techniques (thermal distortion analysis of antennas in space),” *NASA, Langley Research Center, Earth Science Geostationary Platform Technology*, 1989.

[10] S. A. Vorobyov, A. B. Gershman, and Z.-Q. Luo, “Robust adaptive beamforming using worst-case performance optimization: A solution to the signal mismatch problem,” *IEEE Transactions on Signal Processing*, vol. 51, no. 2, pp. 313–324, 2003.

[11] L. Landau, R. C. de Lamare, and M. Haardt, “Robust adaptive beamforming algorithms using low-complexity mismatch estimation,” in *Proc. of Statistical Signal Processing Workshop (SSP 2011)*, 2011, pp. 445–448.

[12] R. Lorenz and S. Boyd, “Robust minimum variance beamforming,” *IEEE Transactions on Signal Processing*, vol. 53, no. 5, pp. 1684–1696, 2005.

[13] D. Rakhimov, B. Peng, E. Jorswieck, and M. Haardt, “Robust reflective beamforming for non-terrestrial networks under thermal deformations,” in *Proc. of International Conference on Acoustics, Speech, and Signal Processing Workshops (ICASSPW 2023)*, 2023, pp. 1–5.

[14] L. Yan-ping, J. Yan-min, and Z. Chao-zhu, “Robust near-field beamforming with worst case performance based on convex optimization,” in *Proc. of 5th Global Symposium on Millimeter-Waves*, 2012, pp. 608–611.

[15] Y. Zheng, R. Goubran, and M. El-Tanany, “Robust near-field adaptive beamforming with distance discrimination,” *IEEE Transactions on Speech and Audio Processing*, vol. 12, no. 5, pp. 478–488, 2004.

[16] H. Van Trees, *Optimum array processing*. John Wiley & Sons, Inc., 2001.

[17] S. Boyd and L. Vandenberghe, *Convex optimization*. Cambridge Univ. Press, 2004.

[18] J. Li and P. Stoica, *Robust adaptive beamforming*. Wiley, 2005.